Journal of Applied Sciences and Nanotechnology

Journal homepage: jasn.uotechnology.edu.iq

Refractory Mullite Phase Enhancement in Silicon Carbide/Kaolin Composites

Safa Luay Jasim*, Shihab A. Zaidan, Enas Muhi Hadi

Department of Applied Science, University of Technology – Iraq

A R T I C L E I N F O

Article history:
Received: January, 24, 2024
Accepted: April, 24, 2024
Available online: September, 10, 2024

Keywords:
Silicon Carbide,
Kaolin,
Mullite phase

Corresponding Author:
Safa Luay Jasim
safaluay194@gmail.com

A B S T R A C T

Refractory ceramics were produced using silicon carbide (SiC) as the main component in combination with different weight percentages of Iraqi white kaolin (20%, 40%, 60% and 80%). Two different weight percentages of alumina (5% and 10%) were then added to each SiC-kaolin mixture. The samples were effectively mixed, molded, dried and fired at 1300 °C. The structural and physical properties were measured, including X-ray diffraction, apparent porosity, water absorption and thermal conductivity. X-ray diffraction showed that the addition of Al_2O_3 to the SiC-kaolin composite increased the mullite phase by interacting with the excess silica formed during the firing of kaolin or with the silica formed during the oxidation of SiC. The increase in kaolin content in the composite without alumina was accompanied by a decrease in physical properties, as the apparent porosity decreased from 30.17% to 17.95% and the water absorption from 16.31% to 7.07%. The addition of 80 wt.% kaolin led to a decrease in thermal conductivity from 35 to 15 W/m.K. The addition of 10 wt% Al_2O_3 also reduced the apparent porosity and water absorption to 13.85% and 5.33% respectively for the (SiC-20 wt% kaolin) sample. The apparent porosity and water absorption of the sample (SiC-80 wt% kaolin) with 10 wt% Al_2O_3 reached the lowest values of 9.44% and 3.55%, respectively. The thermal conductivity decreased from 15 to 12 W/m.K. This study found that adding alumina improves refractory efficiency due to its high melting point, making it ideal for high-temperature applications.

https://doi.org/10.53293/jasn.2024.7257.1271, Department of Applied Sciences, University of Technology - Iraq.

1. Introduction

Silicon carbide (α-SiC Carborundum) is one of the most essential advanced refractories. It is applicable in various parts of thermal systems due to its properties of high thermal shock resistance, high mechanical resistance, and good chemical resistance. The crystalline structure of SiC is mainly composed of covalent bonds, which makes it challenging to sinter [1]. Raising the sintering temperature to complete the process of granular diffusion and complete sintering leads to the oxidation of SiC, and a thin layer of silica is formed [2]. This silicate layer will negatively impact the thermal properties of silicon carbide [3]. SiC is combined with suitable materials, such as kaolin clay ($Al_2O_3.2SiO_2.2H_2O$), to prevent this deterioration. Kaolinite is the main clay mineral in kaolin, and its composition includes varying amounts of other metal oxides, which depend on its geology source [4].

Incorporating kaolin as a plastic material into SiC serves two fundamental purposes: The first purpose is to condense the powder to complete the pressing process by employing the plastic deformation property of clays. The second purpose is to bind the carbide powder by liquid phase sintering during the firing process to obtain a dense mass [5]. The firing process of SiC-Kaolin composites involves the transformation phase, especially in kaolin clays, as follows [6]:

$$\underset{Kaolinite}{3[Al_2O_3.2SiO_2.2H_2O]} \xrightarrow{>1100\,^{\circ}C} \underset{Mullite}{3Al_2O_3.2SiO_2} + \underset{Cristobalite}{4SiO_2} + 6H_2O$$

The mullite phase ($3AlO_3.2SiO_2$) is essential for determining the specifications of clays to be used in the refractory industry, and it consists of approximately 72 % alumina and 28 % silica. The clay specifications increase with alumina increase because it provides more Mullite [7, 8]. Mullite acts as a complement to SiC and supports its thermal properties. The excess of silica (Cristobalite) weakens thermal shock properties because it represents a solidified phase from a liquid state. The composite materials' thermal expansion coefficients must be compatible to prevent the forming of cracks, which weakens the composite's mechanical properties. Practically, Mullite's coefficient of thermal expansion (5.3 μK^{-1} at 0-1000 °C) is almost like that of SiC (4.5 μK^{-1} at 20-700 °C). This compatibility will provide an optimal binding between Mullite and SiC [9]. Kassim KS *et al*. [5] investigated kaolin addition impacts on the properties of silicon carbide with a maximum addition limit of (25 wt%). They observed that the oxidation of silicon carbide resulted in glassy phase formation from excess silica, specifically cristobalite, at high sintering temperatures of up to 1400 °C. At the same time, Sultana F. *et al*. [9] studied different properties of silicon carbide-mullite composites by incorporating coal fly ash as an alumina source to treat the oxidation of silicon carbide. This study aims to prepare refractory ceramics from SiC with different weights of Iraqi white kaolin by adding alumina using an axial compression method.

2. Experimental Procedure

2.1. Materials and specimen preparation

The samples were created using a SiC (99.5 %) and (10 µm < particle size < 38 µm) supplied by Struers company. Kaolin was obtained from the Ministry of Industry and Minerals' Stat Establishment of Geological Survey and Mining provided the kaolin clay. Table 1 shows a high amount of silica and alumina at a lower percentage. Jaw crushers were used to break kaolin stone into small particles, and mortar was used to turn it into fine powder

Table 1: Chemical analysis of kaolin.

Oxide	SiO_2	Al_2O_3	Fe_2O_3	CaO	TiO_2	K_2O	Na_2O	MgO	L.O. I
wt%	49.38	32.72	2.07	1.19	1.08	0.44	0.22	0.18	12.72

. A sieve shaker was then used to sieve the obtained powder (≤ 45 µm). SiC/Kaolin mixtures were fabricated by different SiC/Kaolin ratios (20/80, 40/60, 60/40, and 80/20), as shown in Table 2. To increase the Mullite Phase after firing kaolin, the weight of 5 and 10 wt% of Al_2O_3 (particle size ≤ 30 µm, supplied by Riedel-de Haen) were added to the SiC/Kaolin mixtures (20/80 and 80/20). The disc specimens were produced employing the dry pressing process, the pressing force (50 kN), and the pressing diameter (20 mm). The samples were fired at a controlled temperature of 1300, following a heating program that encompassed the various stages of kaolin's transformation phase, as shown in Table 3

Table 2: Samples codes and weight percentages for all mixtures.

Sample Code	Silicon Carbide (SiC) wt%	Kaolin wt%	Alumina (Al_2O_3) wt%
80S-20K	80	20	-----
60S-40K	60	40	-----
40S-60K	40	60	-----
20S-80K	20	80	-----
80S-20K-5A	95 wt% of 80S-20K		5

80S-20K-10A	90 wt% of 80S-20K	10
20S-80K-5A	95 wt% of 20S-80K	5
20S-80K-10A	90 wt% of 20S-80K	10

Table 3: Sintering stages.

Stage	Temp. °C	Sintering time (hr)	Soaking time (hr)
First	25 – 700	3	2
Second	700 – 1000	2	1
Third	1000 – 1300	1	2

The research methodology is dedicated to adding alumina to increase the amount of Mullite through interactions of alumina with excess silica, as clarified in **Fig. 1**, this demonstrates that combining kaolin and alumina will result (after firing) in a refractory composite of SiC powder bound with Mullite.

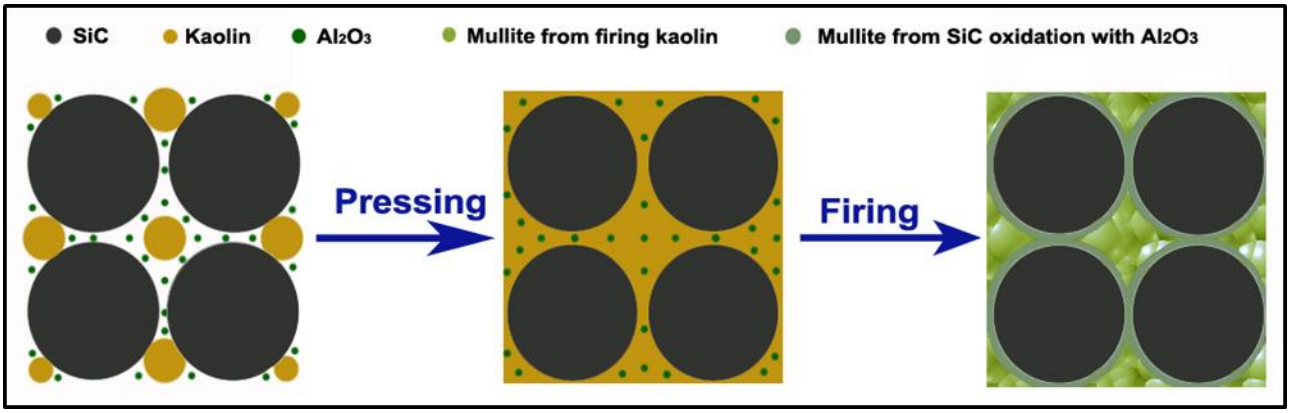

Figure 1: Scheme for preparing a SiC/Kaolin refractory composite.

3. Testing

3.1. Apparent Porosity and Water Absorption:

Apparent porosity (A.P) and water absorption (W.A) were measured for the burnt samples according to standard specifications ASTM (C20) by Archimedes method. The following equations, Eq. (1) and Eq. (2) were used to calculate (A.P) and (W.A) [10, 11].

$$\boldsymbol{A.P\%} = \frac{\boldsymbol{W_s - W_d}}{\boldsymbol{W_s - W_i}} \times \mathbf{100} \qquad (1)$$

$$\boldsymbol{W.A\%} = \frac{\boldsymbol{W_s - W_d}}{\boldsymbol{W_d}} \times \mathbf{100} \qquad (2)$$

W_d: Dry sample mass (g), W_s: Sample mass soaked in water (g), and W_i: Sample mass submerged in water (g).

3.2. Thermal Conductivity:

Thermal conduction is the process of heat transformation from the hotter areas of a substance to its cooler regions. [12]. The basic Eq. (3) for thermal conductivity, which defines this concept, is:

$$\frac{\boldsymbol{dQ}}{\boldsymbol{dt}} = -\boldsymbol{KA}\frac{\boldsymbol{dT}}{\boldsymbol{dx}} \qquad (3)$$

dQ is the quantity of heat that flows to the area (A) in time (dt). The flow heat correlates to the temperature gradient $\left(-\frac{dT}{dx}\right)$. The proportionality factor, known as the thermal conductivity (K), is a material constant. Theoretically, the thermal conductivity coefficient of the composite containing two phases can be characterized. In a previous study, thermal insulation is one of the phases that has a thermal conductivity coefficient (K_A), such as kaolin (~0.4

W/m.K) [13]. Another study (K_M) represents the thermal conductivity coefficient of the second thermally conductive phase (SiC~120 W/mK) [14]. The thermal conductivity coefficient of the composite is calculated from the formula Eq. (4):

$$\boldsymbol{log(K) = (1-f).log(K_M) + f.log(K_A)} \quad (4)$$

f represents the volume fraction of the insulating phase [15].

The thermal conductivity of porous refractories (K_{ref}) is calculated by Eq. (5).

$$\boldsymbol{K_{ref} = K_c\left[\frac{1-P}{1+P}\right]} \quad (5)$$

Kc represents the material thermal conductivity without porosity, and P represents the porosity volume ratio [16][17].Lee's disk method measures the specimen's thermal conductivity, its thickness (ds) is thin compared to its diameter (D). **Fig. 2** shows a diagram of Lee's Disk device for thermal conductivity measurement. Suggesting that the heat flows in the specimen is the quantities average of the heat flowing into and out of it [18], the thermal conductivity is calculated in Eq. (6):

$$\boldsymbol{K\frac{T_U-T_M}{d_S} = h\left[T_M + \frac{2}{r}(d_M + \frac{1}{4}d_S)T_M + \frac{1}{2r}d_S T_U\right]} \quad (6)$$

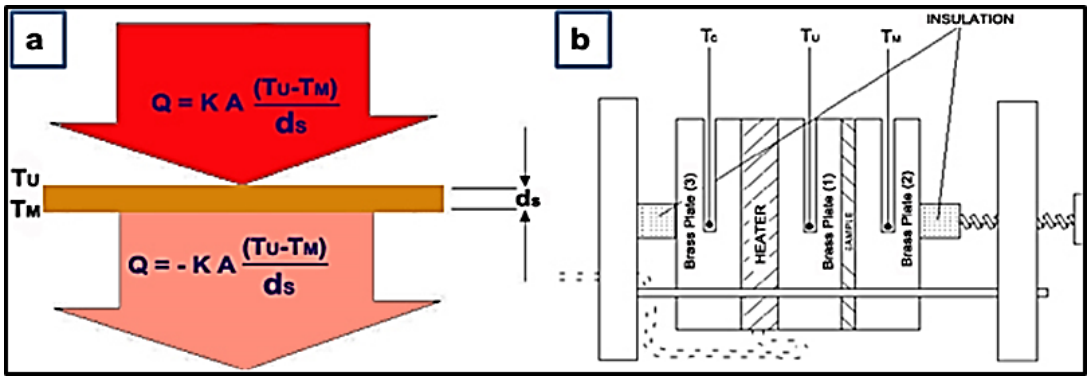

Figure 2: Lee's Disk method for thermal conductivity measurement, (a) Heat transfer (Q), (A) cross the thickness (ds) of the specimen. (b) Diagram of Lee's Disk apparatus.

$T_{U.}$: the disk temperature (U), T_M: the disk temperature (M), the disk radius, d_M: the thickness of the disk M, ds: the disk thickness (S) (specimen), and h: heat loss per second/cm^2 for one degree above the temperature of disk over that of the enclosure, determined from Eq. (7) [12]:

$$\boldsymbol{h = \frac{H_t}{\pi.r\left[(T_C-T_M)r+2\left[d_M.T_M+\frac{1}{2}d_s(T_M+T_U)+d_U T_U+d_C T_C\right]\right]}} \quad (7)$$

dc and T.C. are the thickness and temperature of the disk (C), respectively. Lee's disk system is protected from extraneous impacts by employing glass desiccators. When the system is connected to an electrical power supply, the power is measured in watts by Eq. (8):

$$\boldsymbol{H_t = IV} \quad (8)$$

V: Voltage (6 V), and (I): current equal to 0.25 A. The device's dimensions are r =20.7 mm and d_M= d_U= d_C= 13 mm.

4. Results and Discussion

4.1 SEM Morphology

Fig. 3 shows images taken of the surface of the samples using SEM ((INSPECTS50, Netherlands)). It is clear from them: Image a: Adding a high ratio of kaolin decreases the apparent porosity because the quaternary regular mullite crystals have high compression, with a large percentage of the glassy phase, thereby reducing the porosity. Images b, c, and d: Alumina particles effectively fill the gaps between the SiC and kaolin particles and among other phases, thereby minimizing pore spaces. The small size and uniform distribution of alumina particles allow for effective penetration within the refractory body, enhancing its overall density and structural integrity.

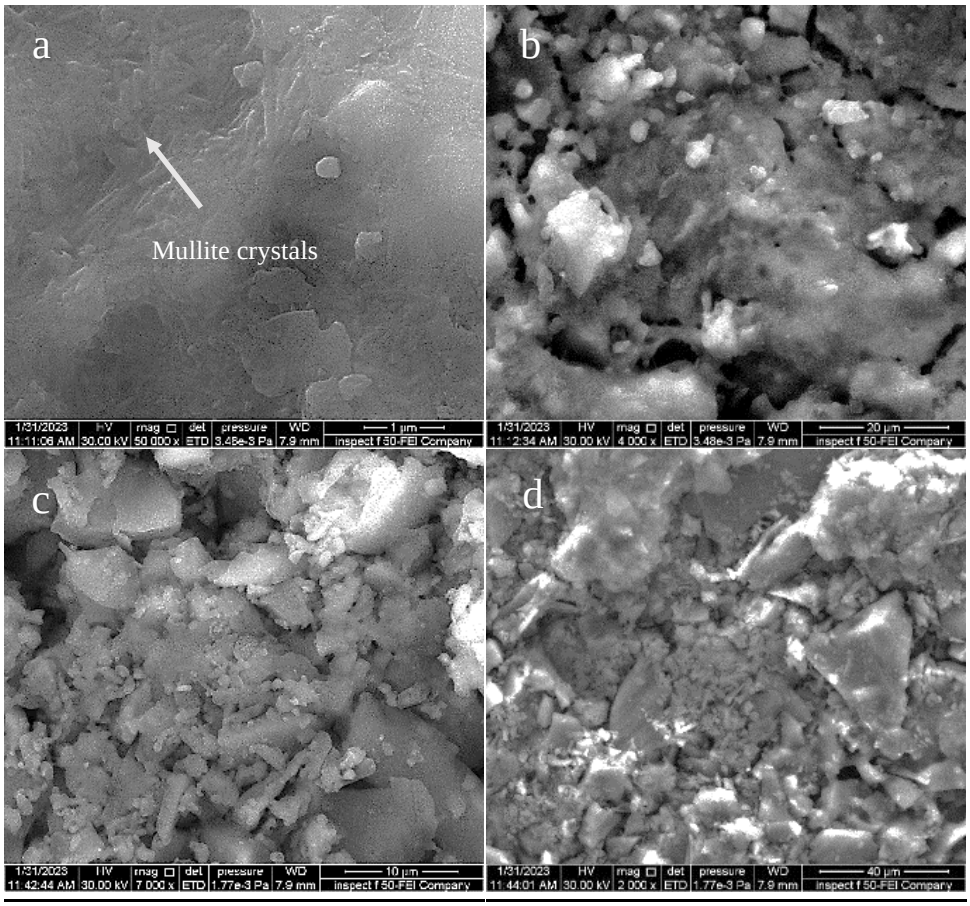

Figure 3: Scanning Electron Microscope of SiC refractory ceramic.

4.2 X-ray diffraction (XRD) Analysis

Two samples of kaolin's crystalline structure were examined before and after the shooting using the X-ray diffraction apparatus SHIMADZU-XRD-6000. The sample 80S-20K represents the kaolin without Al_2O_3, as illustrated in **Fig. 4a**, while **Fig 4b** reveals the sample with 0 % of Al_2O_3. X-ray diffraction results demonstrated that SiC was the main phase, including its typical phases (SiC-4H, 6H, and 3C) [19]. The most distinguished phase among these phases was (SiC-6H), which is related to the Carborundum phase (α-SiC). The fired kaolin products, represented by Mullite ($3Al_2O_3.2SiO_2$) with excess silica, appeared obviously in the diffraction image. Because the utilized kaolin does not contain high percentages of alumina, cristobalite is considered one of the essential oxides, which cooperates with other oxides (except alumina) to form glassy phases that lower the melting temperature of the composite [20]. The presence of flux oxides causes the formation of the mullite phase at an early temperature of lower than 1200°C (lower than the required temperature for mullite formation from alumina-silica, which is about 1550 °C) [21, 22]. Adding alumina had a noticeable effect in increasing the mullite phase peaks while decreasing cristobalite. However, 10 wt% of alumina was insufficient to convert all the cristobalite into Mullite, so the cristobalite phase did not disappear completely. Also, extending the heat treatment time may

increase the cristobalite phase due to the oxidation of SiC. Therefore, increasing the firing temperature or soaking time is ineffective.

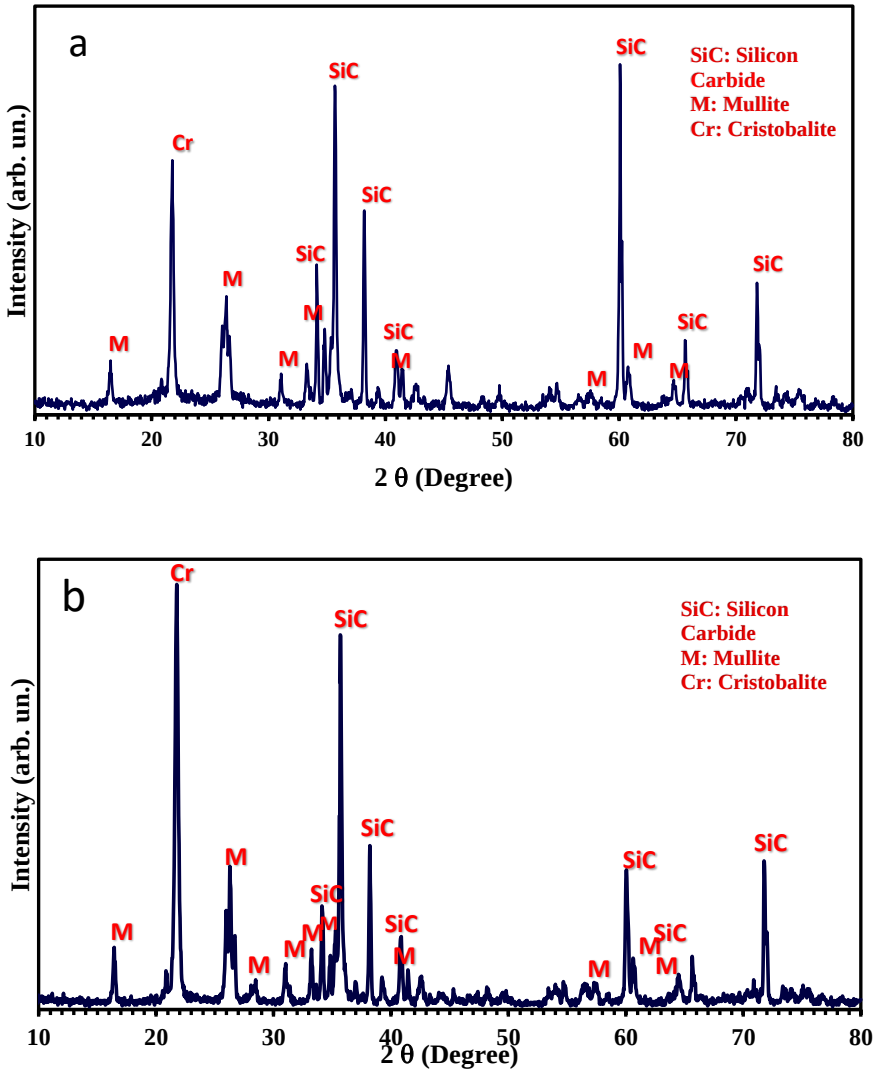

Figure 4: X-ray diffraction analysis of (80S-20K) refractory ceramics: **a**) Without adding alumina, **b**) After adding 10 wt% alumina.

The transformation of kaolinite sheet shapes into needle-like structures of Mullite affects the composite's structure. The Mullite needle-like structures significantly strengthen the composite structure by surrounding the oxidized layer of SiC, similar to the reinforcement by whiskers [23]. Adding alumina enhances mullite formation by interacting with either the oxide layer produced by SiC or interacting with cristobalite, thereby increasing the mullite phase. Therefore, the SiC peaks decreased due to the surface oxidation of SiC powder and the combination with alumina. Additionally, increasing the cristobalite phase peak at the diffraction angle ($2\theta = 21.79°$) may be attributed to the crystallization of silicon oxide and its transformation into the cristobalite phase.

4.3 Apparent Porosity and Water Absorption

Fig. 4 illustrates the porosity of the prepared composite samples (SiC/Kaolin) at a firing temperature of 1300 °C, and atmospheric pressure conditions for two hours. The samples' apparent porosity decreased as the kaolin weight (%) increased. However, the porosity of the prepared sample (80S-20K) without alumina addition was much higher than that of the sample (20S-80K). When kaolin was added, the porosity values decreased from 30.17% to 17.95%, and this can be attributed to the plasticity of the clay, which causes high compaction and thus closes the pores. SiC surface oxidation occurs because of the oxygen in the firing atmosphere and water vapor released from the kaolin

structure during the transformation phase. This oxidation leads to the formation of the glassy phase (SiO_2) and, thus, increased condensation between the SiC grains with the kaolin increasing. Thereby decreasing the porosity [23]. Likewise, porosity decreased with the percentage increase of added size alumina to the two samples, as in **Fig. 5**. The addition of 10% alumina to the sample (80S-20K) resulted in a significant porosity percentage decreasing from 30.17 % to 13.85 %. Also, the apparent porosity decreased from 17.95% to 9.44% for the (20S-80K) sample. It is possible to enhance the formation of Mullite by reacting SiO_2, which results from the oxidation of SiC, with added alumina. This process can create a layer of Mullite around the SiC grains. Moreover, the melting temperature of SiC was higher than the melting temperature of SiO_2. While the Mullite's viscosity reduced, this led to the grains' convergence and the filling of the interstitial pores [24].

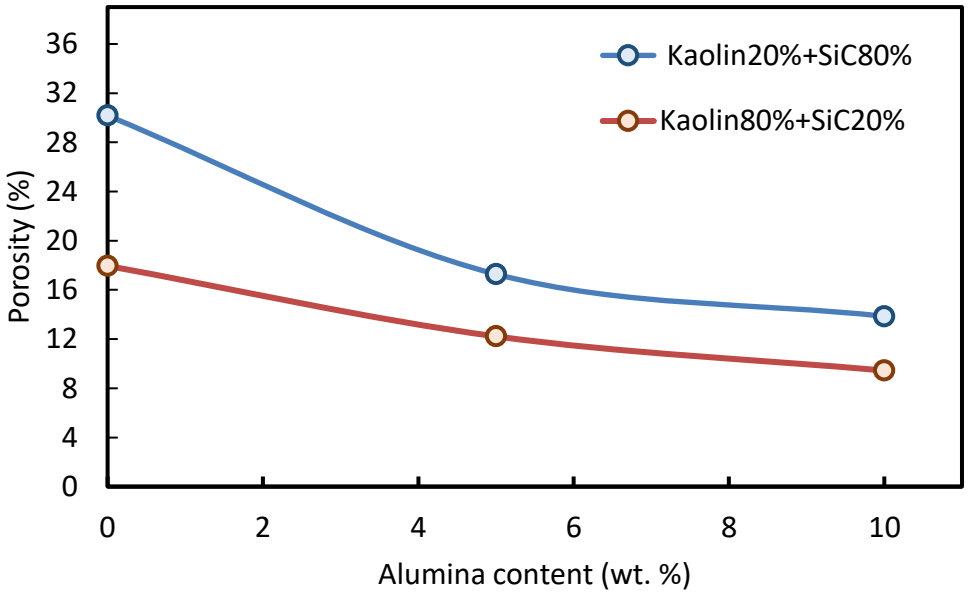

Figure 5: Dependence of apparent porosity of SiC/Kaolin composites.

The water absorption percentage is like that of apparent porosity. Both properties relate to the amount of water penetrating the ceramic body through open pores only. The required water absorption for each application defines most technical standards for ceramic and refractory materials. Generally, **Fig. 6** indicates a reduction in water absorption as the kaolin percentage increases, approaching 16.31% for the composite (80S-20K). The absorption rate gradually decreased to 7.07 % for the composite (20S-80K). The findings in **Fig. 7** indicate the effect of adding alumina. The absorbance dropped with alumina addition, reaching 5.33% when 10% alumina was added to the combination (80S-20K). When 10% alumina was added to the sample (20S-80K), it reached its lowest level of 3.55%.

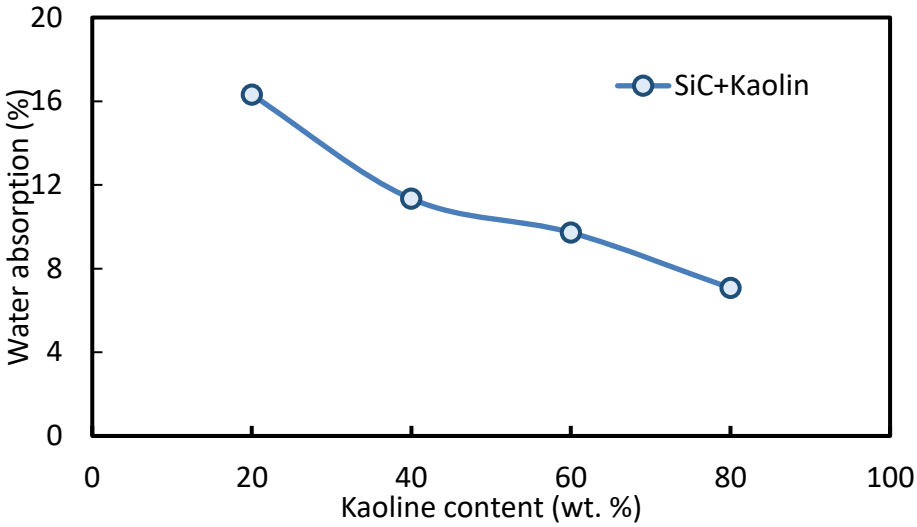

Figure 6: Dependence of water absorption of SiC/Kaolin composites.

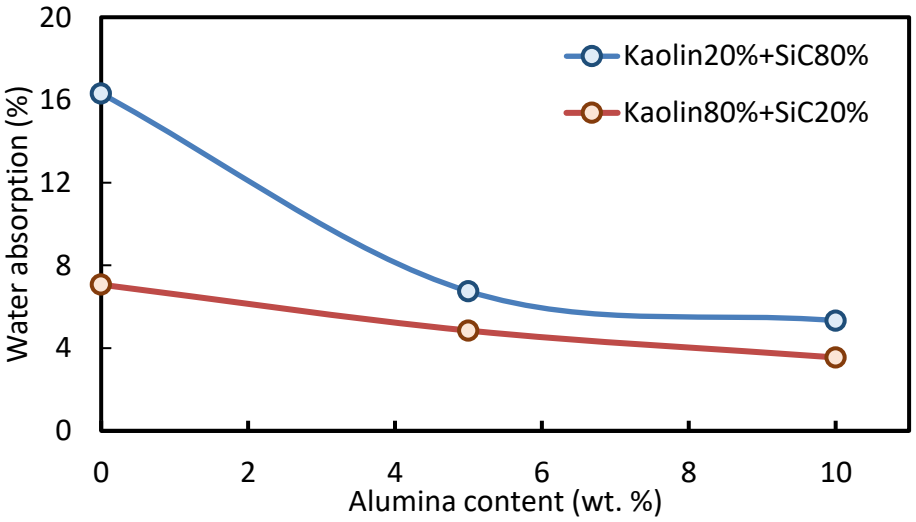

Figure 7: Dependence of water absorption of SiC/Kaolin with Alumina additives.

4.4 Thermal conductivity

The two main factors controlling thermal conductivity values are the composite components' thermal conductivity and porosity coefficient. Formula (4) describes the effect of the components and may be used to estimate the thermal conductivity coefficients of composites. These results show that increasing the volume fraction of the insulating phase in the composite decreases the thermal conductivity coefficient, which agrees with the results reported in **Fig. 8**. The results revealed that the thermal conductivity reduced from 35 W/m.K (for 80S-20K) to 15 W/m.K (for 20S-80K), a reduction of almost half. Despite the decrease in porosity, which should theoretically increase thermal conductivity according to formula (5), the impact is less significant than the decrease caused by the differing thermal conductivity values of the materials forming the ceramic composite. The addition of alumina increased the mullite phase due to the reaction of excess SiO_2 resulting from firing kaolin or alumina with silicon oxide, which led to the oxidation of SiC. Specifically, the addition of alumina caused thermal conductivity reduction due to the increased mullite phase [13]. Consequently, the glass phase declined, resulting in thermal conductivity values of 27 W/m·K for the mixture (80S-20K) and 12 W/m·K for the mixture (20S-80K) after adding 10 wt% of alumina, as shown in **Fig. 9**. In comparison with Sultana F *et al*. [9], the values reported for SiC composites bonded with clay and dispersed with alumina are consistent with those of silicon carbide composites prepared by adding coal fly ash, which have a thermal conductivity of 17 W/m·K.

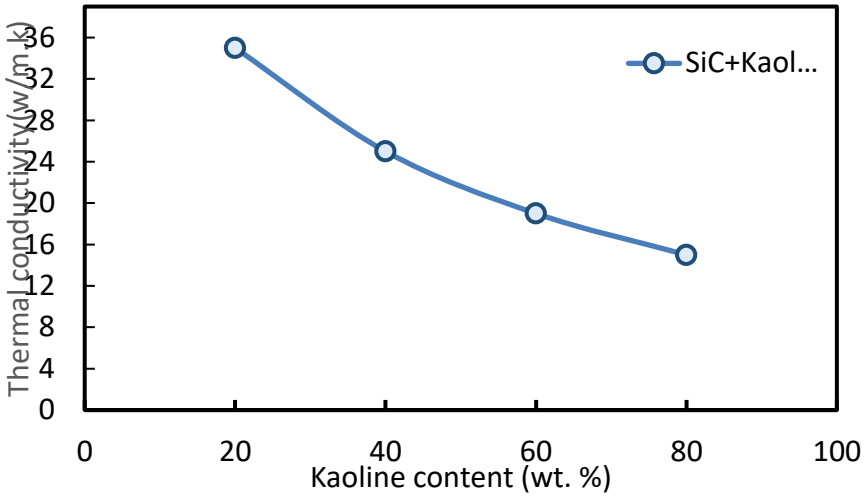

Figure 8: Thermal conductivity of SiC/Kaolin composites.

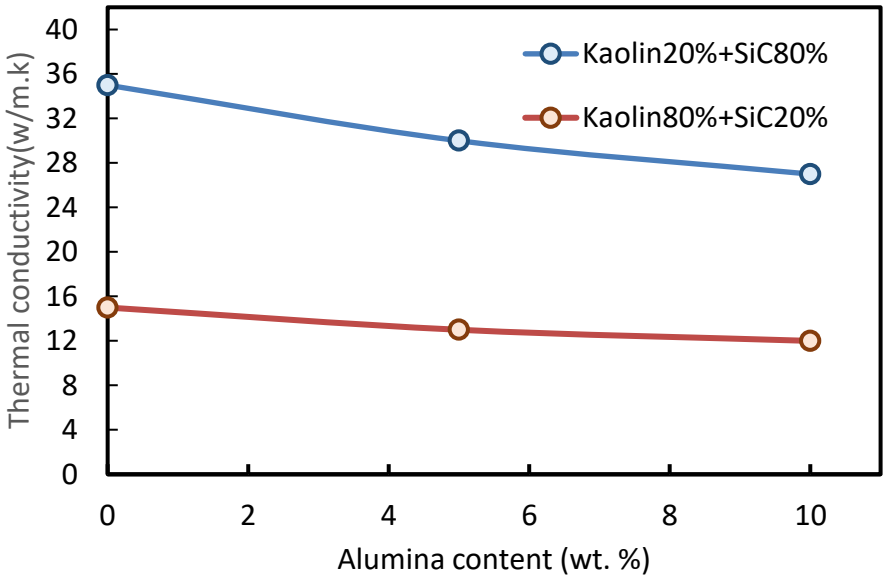

Figure 9: Thermal conductivity of SiC/Kaolin with Alumina additives.

5. Conclusions

Despite the significant differences between traditional kaolin clay and advanced silicon carbide properties, they are compatible when mixed in refractory composites (SiC/Kaolin). This compatibility was evident as the prepared samples showed no macroscopic defects. The addition of alumina contributed to the increase of the mullite phase through its interaction with cristobalite, which forms from firing kaolin, or through its interaction with silicon oxide, which results from the oxidation of SiC within the boundaries of the sample surface. Kaolin provides the plasticity required to achieve the dry pressing process, maximum compaction of powders, and high homogeneity in the dimensions of samples. Because of the significant variation in the values of the thermal conductivity coefficients of the refractory composite (SiC/Kaolin) components ($K_{SiC} >> K_{Kaolin}$), its effect is higher than that of porosity in decreasing the thermal conductivity coefficient as the percentage of kaolin increases. The Mullite resulting from the reactions of added alumina and formation of silica at a temperature of 1300 °C, which is lower than that necessary for the reaction of the mullite components ($3Al_2O_3.2SiO_2$), which reaches 1550 °C as described in the Al_2O_3-SiO_2 phase diagram. The increase in Mullite reduced the glassy phase resulting from the interaction of silica with fluxes oxides (K_2O, CaO, Na_2O…). Therefore, the refractory tolerance of (SiC/Kaolin) composites improved at higher temperatures. Consequently, these refractories can be applied in thermal systems as thermally resistant material.

Conflict of Interest

The authors declare that they have no conflict of interest.

References

[1] A. J. Ruys, Silicon Carbide Ceramics: Structure, Properties and Manufacturing. Elsevier, 2023.

[2] S. Chen et al., "Static and dynamic oxidation behaviour of silicon carbide at high temperature," *J. Eur. Ceram. Soc.*, vol. 41, no. 11, pp. 5445–5456, 2021. DOI: 10.1016/j.jeurceramsoc.2021.05.033.

[3] Y. Shinoda, D. B. Marshall, and R. Raj, "Oxidation, mechanical and thermal properties of hafnia–silicon carbide nanocomposites," *J. Eur. Ceram. Soc*., vol. 34, no. 7, pp. 1783–1790, 2014. DOI: 10.1016/j.jeurceramsoc.2013.12.024.

[4] B. X. Lorentz, Low-Grade kaolin clay natural resource for use as a supplementary cementitious material in structural concrete elements, University of South Florida, 2020.

[5] K. S. Kassim, S. A. Z. Al-Juboori, and A. M. Al Sheikh, "Mechanical strength of silicon carbide bonded with Iraqi clays," *Eng. Technol. J.*, vol. 29, pp. 745–752, 2011.

[6] B. S. Gonidanga, D. Njoya, G. Lecomte-Nana, and D. Njopwouo, "Phase transformation, technological properties and microstructure of fired products based on clay-dolomite mixtures," *J. Mater. Sci. Chem. Eng.*, vol. 7, no. 11, pp. 1–14, 2019. DOI: 10.4236/msce.2019.711001.

[7] R. Roy, D. Das, and P. K. Rout, "A review of advanced mullite ceramics," *Eng. Sci.*, vol. 18, pp. 20–30, 2021. DOI: 10.11648/j.eng.20211801.13.

[8] H. Jabbar, E. Muhi, and T. Hussien, "Preparing and Investigating the Structural Properties of Porous Ceramic Nano-Ferrite Composites," *J. Appl. Sci. Nanotechnol.*, vol. 3, no. 1, pp. 34–41, 2023.

[9] F. Sultana, N. Yang, C. Xu, J. Monroe, and A. El-Ghannam, "Synthesis and characterisation of functionally graded SiC-mullite thermal material," *J. Solid State Chem.*, vol. 330, p. 124414, 2024. DOI: 10.1016/j.jssc.2023.124414.

[10] ASTM C 326, Standard Test Method for Drying and Firing Shrinkages of Ceramic Whiteware Clays, ASTM International, West Conshohocken, USA, 2003.

[11] ASTM C 20, Standard Test Methods for Apparent Porosity, Water Absorption, Apparent Specific Gravity, and Bulk Density of Burned Refractory Brick and Shapes by Boiling Water, ASTM International, West Conshohocken, USA, 2005.

[12] S. Zaidan, Bonded Silicon Carbide with Iraqi Clays, University of Technology-Iraq, 2005.

[13] A. Michot, D. S. Smith, S. Degot, and C. Gault, "Thermal conductivity and specific heat of kaolinite: Evolution with thermal treatment," *J. Eur. Ceram. Soc.*, vol. 28, no. 14, pp. 2639–2644, 2008. DOI: 10.1016/j.jeurceramsoc.2008.03.027.

[14] Y. Zhou, K. Hirao, K. Watari, Y. Yamauchi, and S. Kanzaki, "Thermal conductivity of silicon carbide densified with rare-earth oxide additives," *J. Eur. Ceram. Soc.*, vol. 24, no. 2, pp. 265–270, 2004. DOI: 10.1016/S0955-2219(03)00287-2.

[15] N. F. Uvarov, "Estimation of composites conductivity using a general mixing rule," *Solid State Ionics*, vol. 136, pp. 1267–1272, 2000. DOI: 10.1016/S0167-2738(00)00435-0.

[16] S. A. Zaidan, "Manufacturing of porous refractories from Iraqi Kaolin by adding expanded polystyrene waste," *Iraqi J. Phys.*, vol. 16, no. 37, pp. 118–126, 2018.

[17] C. B. Carter and M. G. Norton, Ceramic Materials: Science and Engineering, vol. 716, Springer, 2007. DOI: 10.1007/978-0-387-46270-7.

[18] H. A. Sharhan, Z. N. Rasheed, and J. K. Oleiwi, "Synthesis and Physical Characterisation of PMMA/PP and PMMA/PAN Composites for Denture Applications," *J. Appl. Sci. Nanotechnol.*, vol. 1, no. 3, pp. 13–23, 2021.

[19] A. L. Ortiz, F. Sanchez-Bajo, F. L. Cumbrera, and F. Guiberteau, "X-ray powder diffraction analysis of a silicon carbide-based ceramic," *Mater. Lett.*, vol. 49, no. 2, pp. 137–145, 2001. DOI: 10.1016/S0167-577X(00)00323-4.

[20] F. H. Gata and E. MHUI, "Study of the Mechanical and Thermal Properties of Refractory Mortars from Kaolin and Bentonite," *J. Appl. Sci. Nanotechnol.*, vol. 2, no. 1, pp. 69–79, 2022.

[21] L. Andrini et al., "Extended and local structural description of a kaolinitic clay, its fired ceramics and intermediates: an XRD and XANES analysis," *Appl. Clay Sci.*, vol. 124, pp. 39–45, 2016. DOI: 10.1016/j.clay.2016.02.007.

[22] H.-J. Kleebe, F. Siegelin, T. Straubinger, and G. Ziegler, "Conversion of Al2O3–SiO2 powder mixtures to 3:2 mullite following the stable or metastable phase diagram," *J. Eur. Ceram. Soc.*, vol. 21, no. 14, pp. 2521–2533, 2001. DOI: 10.1016/S0955-2219(01)00055-0.

[23] G. Chen et al., "Design and direct preparation of a novel silicon carbide support for zeolite membrane," *Appl. Water Sci.*, vol. 12, no. 11, p. 249, 2022. DOI: 10.1007/s13201-022-01681-4.

[24] J.-H. Eom, Y.-W. Kim, S.-K. Woo, and I.-S. Han, "Effect of submicron silicon carbide powder addition on the processing and strength of reaction-sintered mullite-silicon carbide composites," *J. Ceram. Soc. Japan*, vol. 117, no. 1364, pp. 421–425, 2009. DOI: 10.2109/jcersj2.117.421